





Investigation into a hybrid mooring system with hydrodynamic response and mooring tension from a DeepCwind floating wind turbine

Arman Aghaei Ganjgani¹, Hassan Ghassemi² , Mahmoud Ghiasi³

¹  <https://orcid.org/0000-0002-8541-4813>

²  <https://orcid.org/0000-0002-6201-346X>

³  <https://orcid.org/0000-0002-7824-7164>

Amirkabir University of Technology, Department of Maritime Engineering
Marine and Hydrokinetic Energy Group, Tehran, Iran
e-mails: ¹arman.sspp1993@aut.ac.ir, ²gasemi@aut.ac.ir, ³mghiasi@aut.ac.ir
 corresponding author

Keywords: DeepCwind platform, BEM, buoys, clump weight, catenary mooring line

JEL Classification: C63, C61, P18

Abstract

This paper investigates the effect of buoys and a clump weight on the mooring lines and the dynamic response of the floating platform. The full-scale of the OC4-DeepCwind semisubmersible FOWT platform is analyzed using the boundary element method (BEM) with ANSYS-AQWA software, when considering regular wave conditions. Platform motions and mooring line tension in the surge, heave, and pitch are presented and discussed in the time domain analyses (TDA) and frequency domain analyses (FDA). Validation is performed by comparison of the platform motion RAO and the fairlead tension RAO magnitudes in the surge, heave, and pitch (for both numerical and experimental data) under seven sea states' regular waves. The results show that increasing the number of buoys at a constant volume decreases the surge and pitch motion amplitude, while the heave motion increases slightly. Adding the buoy and clump weight (type 1) to the mooring line reduces the oscillation amplitude tension. In addition, raising the number of buoys increases the oscillation tension.

Introduction

Mooring lines systems have been used to provide the necessary restoring force that acts against environmental loadings to minimize the floating offshore structure motions. As the water depth increases, the weight of the mooring line that consists of chains or cables became too heavy, and the vertical forces from the restraints on the floating platform increase. In the catenary mooring system, part of the mooring line is rested on the seabed. The restoring force is generated when the excursion or vessel motion lifts the catenary mooring system. The buoys and clump weights used in the suspended portion of the mooring

system can effectively reduce the platform response and mooring lines tension (Liu et al., 2019).

Many researchers have investigated the effect of the buoy and clump weight on the mooring line system and floating platform response in recent years. Yuan et al. proposed a hybrid mooring system with several clump weights and buoys to optimize the position and volume of the buoys, based on the mooring line tension. In their work, Morrison's equation was used to calculate the hydrodynamic loads (Yuan, Incecik & Ji, 2014). Brommundt et al. developed a numerical tool to optimize the catenary mooring system of a semisubmersible wind turbine platform with two different depths (i.e. 75 m and

330 m). Mooring line length, angle, and horizontal distance between the anchor and fairlead were also investigated (Brommundt et al., 2012). Fitzgerald and Bergdahl (2007) used a buoy-attached mooring as a wave energy converter at a water depth of 50 m, which indicated that the buoy may reduce cable weight, induce mooring loads, and affect floater motion. Hybrid mooring concepts, such as clump weight and buoy, have also been developed (Hall & Goupee, 2015). Hall and Goupee (2015) introduced a lumped-mass model to evaluate the dynamics response of the mooring line system for DeepCwind semisubmersible FOWT. The obtained results were compared with experimental data from a scale model (Hall & Goupee, 2015). Qiao et al. (2014) have investigated the effects of buoys on the dynamic response of mooring lines and platform motion numerically (Qiao & Ou, 2013). Mavrakos and Chatjigeorgiou (1997) used the frequency domain analyses (FDA) and time domain analyses (TDA) to examine the mooring line motion and tension, including different buoy sizes and locations in deep water (Mavrakos & Chatjigeorgiou, 1997). Mavrakos et al. (Mavrakos et al., 1991) studied the benefit of attaching buoys to the mooring line and confirmed that the mooring line dynamic could be reduced when the size, number, and location of the buoys are chosen correctly. Hordvik (2011) carried out optimization of the mooring system design, using quasi-static and dynamic analysis in shallow water, for a floating wind turbine with three catenary mooring lines. In this work, three types of mooring systems consisting of distributed mass, clump weight, and buoyancy element schemes have been considered for evaluating the system behavior (Hordvik, 2011). Benassai et al. (2014) compared the motion control performance of the catenary mooring, and the tension line mooring systems for the Dutch tri-floater wind turbine, at a water depth between 50 m and 200 m that minimizes the mooring line weight. Both operational and extreme load cases are considered, the weight of the chain cable and steel wire rope are compared for different water depths (Benassai et al., 2014). Vicente et al. compared the mooring configurations of a floating-point absorb consisting of catenary chain with and without additional clump weight or buoy (Vicente, Falcão & Justino, 2011). The results showed that the maximum horizontal motion and energy absorption power are less sensitive to different arrangements of the buoys and clump weights compared to average and maximum mooring line tension. Ghafari and Dardel investigated the effect of diameter, and the number

of buoys, on the response of the Amirkabir semisubmersible drilling platform using the boundary element method (BEM). The results show that increasing the number of buoys decreases the amplitude of the surge motions, while increasing the heave and pitch (Ghafari & Dardel, 2018).

We opened a new group called Marine and Hydrokinetic Energy (MHK) at the Amirkabir University of Technology (AUT) and we are working on different types of wave energy converters and their platforms. The purpose of this paper is to investigate the hydrodynamic response of the DeepCwind semisubmersible floating offshore wind turbine (FOWT) platform, which consists of three mooring lines that are divided into three segments with an intermediate buoy and clump weight. Simulations were performed in ANSYS AQWA under regular airy wave conditions. Fairlead tension and platform motions are presented and discussed in three directions (i.e. surge, heave, and pitch).

Governing equations

The governing equations, including potential flow theory, have been used, and three-dimensional radiation/diffraction theory has been used to estimate the wave force that acts on the rigid floating platform. The potential flow expression includes the first-order incident wave potential, the corresponding diffracted wave potential, and the radiation wave potential due to the j -th motion with unit motion amplitude (Bartrop, 1998). The hydrodynamic loads, the motion responses, and mooring forces responses are obtained using three-dimensional radiation/diffraction theory and Morison element theory. The floating object's fluid flow field is defined using the Laplace equation as the governing equation. A boundary integration method calculates the fluid velocity potential function with boundary conditions (Ghafari & Dardel, 2018). The Morison element models the mooring line as a chain under various external factors. This includes the external hydrodynamic, structural, and inertia loadings. Considering the hydrodynamics interaction among M floating bodies, and using frequency-dependent coefficients, the linear equation of motion is expressed as follow:

$$\left[-\omega_e^2(M_s + M_a) - i\omega_e C + K_{hys} \right] [x_{jm}] = [F_{jm}] \quad (1)$$

Here, M_s is a $6M \times 6M$ structure mass matrix and $M_a = [A_{jm, kn}]$ and $C = [B_{jm, kn}]$ are the $6M \times 6M$ hydrodynamic added mass and damping matrices, respectively,

which consist of hydrodynamic interaction coupling components between M structures; K_{hys} is the hydrostatic stiffness matrix. Moreover, F_{jm} is the total forces and moments, while subscripts j and k correspond to the motion modes and the subscripts m and n refer to the m -th and n -th structure, respectively. By defining an integral convolution form, the equation of motion may be described as (Cummins, 1962):

$$\{m + A_{\infty}\} \ddot{X}(t) + c \dot{X}(t) + K X(t) + \int_0^t R(t-\tau) \dot{X}(\tau) d\tau = F(t) \quad (2)$$

where R is the velocity impulse function matrix and $F(t)$ is the total force, which includes the mooring force and first- and second-order wave force. For the hydrodynamics analysis, the second-order wave force should be considered as one of the important loads (Motallebi et al., 2020). The significance of the second-order wave force on the floating wind platform has been demonstrated both computationally and experimentally (Li et al., 2017). Refer to (Ghafari et al., 2019) for additional information on the mooring force equations.

DeepCwind characteristics

The present result is compared to experimental data from the DeepCwind semisubmersible floating platform, which is used in the studies by Coulling et al. (2013) and shown in Figure 1. The DeepCwind

Table 1. Characteristics of the DeepCwind semisubmersible platform

Properties	Value	Unit
Depth to platform base below SWL (total draft)	20	m
Water depth	200	m
Water mass density	1025	kg/m ³
Elevation of the main column above SWL	10	m
Elevation of the offset column above SWL	12	m
Space between offset columns	50	m
Diameter of main column	6.5	m
Diameter of offset columns	12	m
Diameter of base columns	24	m
Dimeter of pontoon and cross bracings	1.6	m
Displacement	13 986.8	m ³
Center of mass (CM) location below SWL	14.4	m
Platform roll inertia about CM	8.011×10^9	kg/m ²
Platform pitch inertia about CM	8.011×10^9	kg/m ²
Platform Yaw inertia about platform centerline	1.391×10^9	kg/m ²

semisubmersible floating platform model has been tested at the Maritime Research Institute Netherlands offshore wind/wave basin, by the University of Maine DeepCwind program (Coulling et al., 2013). It should be mentioned here that the experimental model for the DeepCwind semisubmersible platform was evaluated in 1:50 scale model experiments. Tables 1 and 2 show the characteristics of the DeepCwind semisubmersible floating platform.

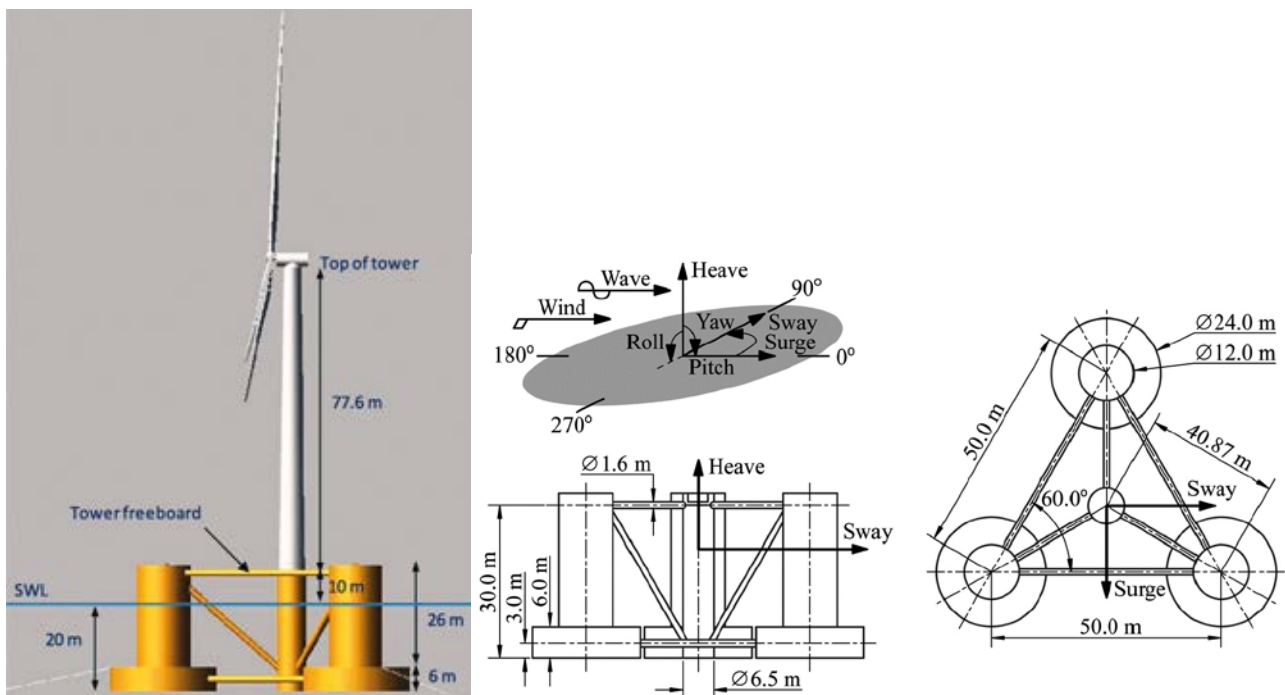


Figure 1. OC4 DeepCwind semisubmersible design by Coulling et al. (2013)

The purpose of this paper is to investigate the hydrodynamic behavior of the mooring lines on the DeepCwind semisubmersible FOWT platform. The mooring lines consist of three catenary steel chains at an angle of 120 degrees to each other; it is designed for a water depth of 200 m. Each nonlinear catenary mooring line is divided into intermediate buoys and a clump weight.

Figure 2 shows the platform orientation and the mooring line configuration. While the mooring line properties are listed in Table 2.

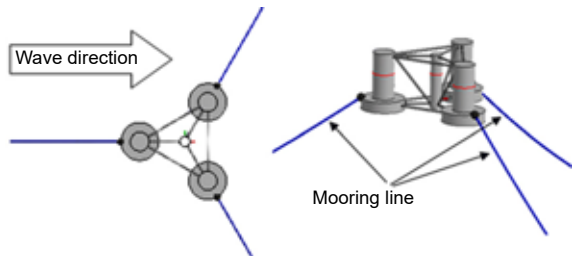


Figure 2. Arrangement of the mooring lines

Table 2. Mooring line properties

Properties	Value	Unit
Number of mooring lines	3	–
Angle between lines	120	degree
Radius to anchors from platform center line	837.6	m
Radius to fairleads from platform center line	40.868	m
Unstretched line length	835.5	m
Mooring line diameter	0.0766	m
Equivalent mooring line mass density	113.35	kg/m
Equivalent mooring line mass in water	108.63	kg/m
Extensional stiffness	753.6×10^6	N

Results and discussion

Validation

The validation is divided into two main steps: (1) the platform RAO response and (2) the fairlead tension RAO under seven regular wave environments. The present numerical result is obtained from potential theory using the BEM method and it is compared to experimental data from Coulling et al. (2013). Based on the convergence analysis results, a maximum element size of 1.8 m is obtained, including the 7800 panels and 5400 diffracting elements shown in Figure 3.

Seven different regular waves were considered, and the platform response was investigated to validate the numerical results of the RAO response motions and the mooring tension. Table 3 shows the

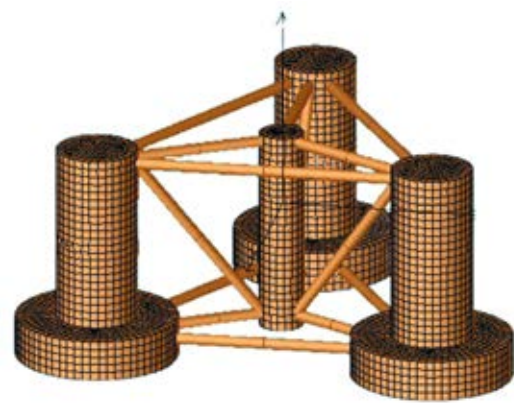


Figure 3. Mesh of the DeepCwind semisubmersible

Table 3. Sea states characteristics (Coulling et al., 2013)

Sea state	A (m)	T (s)
LC1	0.96	7.50
LC2	3.79	12.10
LC3	3.57	14.30
LC4	3.79	20.00
LC5	5.15	12.10
LC6	5.37	14.30
LC7	5.56	20.00

selected sea states for regular waves defined by its period, T , and amplitude, A .

Figure 4 compares the numerical and experimental data for the platform motion RAO in the surge, heave, and pitch under the seven different sea states' regular waves. The root mean squared error (RMSE) for the DeepCwind semisubmersible floating platform shows a relatively good agreement between the numerical results and measurement data for all three motions (Table 4).

Table 4. Root mean squared error (RMSE) for the seven regular waves

Sea state	Surge (m/m)		Heave (m/m)		Pitch (deg/m)	
	Exp	Num	Exp	Num	Exp	Num
Regular wave 1	0.17	0.153	0.07	0.063	0.25	0.207
Regular wave 2	0.58	0.62	0.3	0.28	0.259	0.15
Regular wave 3	0.75	0.747	0.29	0.178	0.23	0.18
Regular wave 4	0.99	0.911	1.29	0.896	0.31	0.28
Regular wave 5	0.66	0.622	0.34	0.282	0.3	0.27
Regular wave 6	0.77	0.748	0.37	0.182	0.27	0.21
Regular wave 7	1.01	0.913	1.2	0.894	0.42	0.31
	RMSE	0.268	RMSE	0.295	RMSE	0.237

Figure 5 compares the present numerical results and experimental data of the fairlead tension RAO magnitudes for different sea states' regular waves.

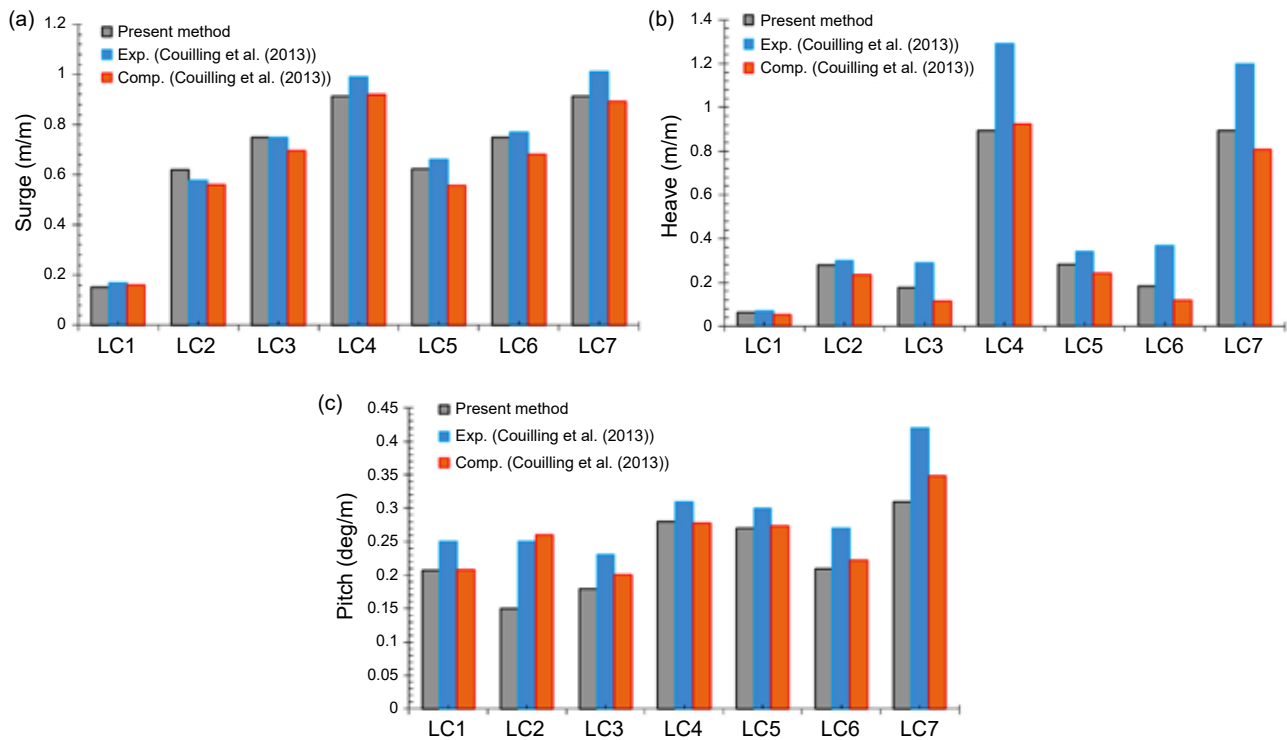


Figure 4. Comparison of the DeepCwind RAO (a) surge, (b) heave, and (c) pitch

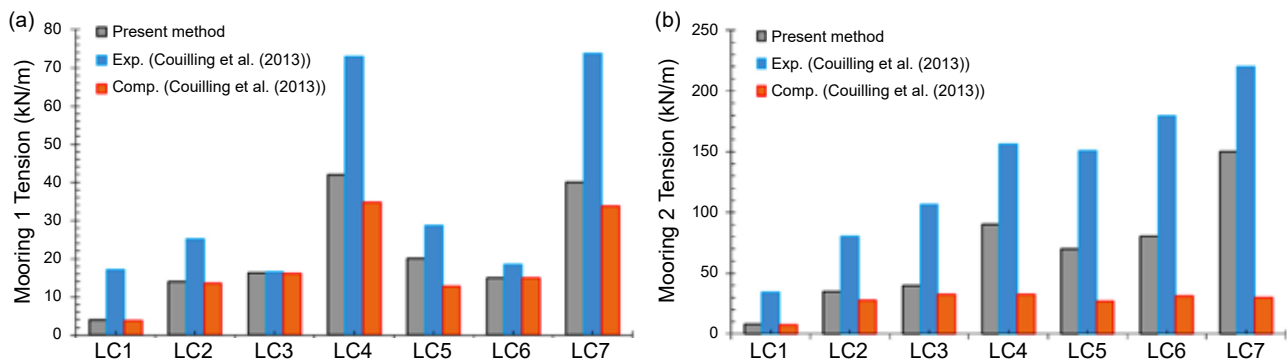


Figure 5. Comparison of the fairlead tension RAO magnitudes for (a) mooring line 1 and (b) mooring lines 2

It can be seen that the numerical results are in a reasonably good agreement with the experimental data. At the amplitude of the wave height and period, mooring line 1 experiences more tension. It should be noted that similar results were obtained due to the symmetry between mooring lines 2 and 3. However, in the present study, only mooring line 2 is given. It can be observed that the DeepCwind test data and the numerical simulation results are in relatively good agreement.

Following validation of the numerical model that uses the BEM with regular waves, a case when no wind is present is tested. Figure 6 depicts the platform RAO in regular waves with periods ranging from 5 s to 25 s, which are obtained from the AQWA and then compared to the test data and FAST results published by Coulling et al. (2013). As can be seen,

the RAOs are consistent with the FAST data, and a similar behavior is shown in the heave, pitch, and surge motions. However, close to the natural heave frequency, a more significant heave motion was estimated by the AQWA.

The new mooring system

To arrange a decrease in the vertical component of the mooring tension at the top of the mooring line, a series of buoys with a constant volume and a clump weight are attached to each mooring line. Keeping the arrangements of the mooring system constant, four types of buoys and a clump weight are connected in the mooring line, and the locations of the buoys are 150 m, 180 m, 210 m, and 240 m, and the clump weight is a distance of 650 m, from the

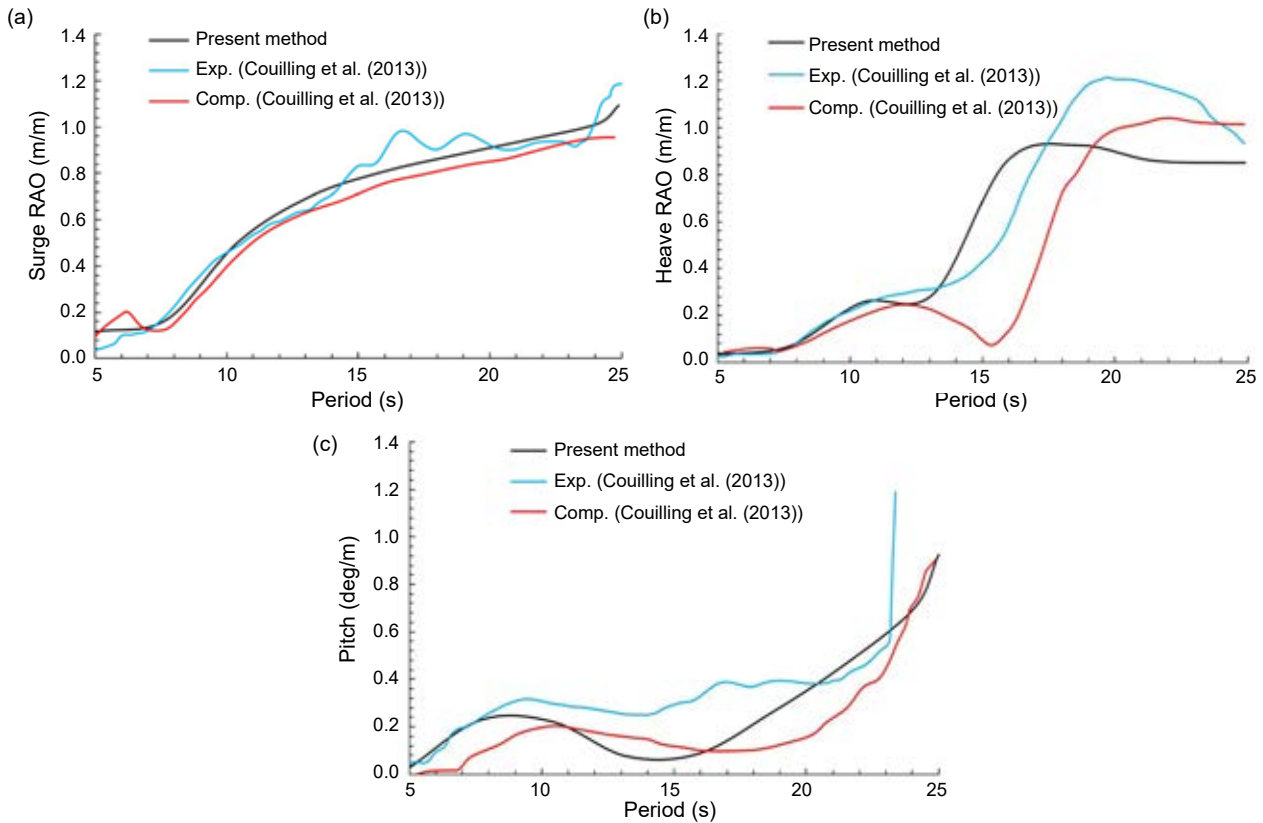


Figure 6. Comparison of the RAO response between the test data (Coulling et al., 2013) and the present study: (a) surge, (b) heave, and (c) pitch

platform. Figure 7 shows the position of the buoys and a clump weight for one of the mooring systems arrangements. A couple of mooring lines with clump weights and buoys constitute a new hybrid system. The buoyancy of these buoys counteracts some of the effects of gravity and, as a result, the tension on each mooring line can be decreased. Consequently, the motions of the platform might also be reduced. Thus, the horizontal restoring force provided by the line can be increased, while the restoring forces in the vertical direction will be reduced. The mooring system properties are summarized in Table 5.

The time responses and frequency responses of the platform’s surge, heave, and pitch motions by the mooring system, with a clump weight and buoy statistical variability of the maximum, minimum, and average values of the motion responses and tension

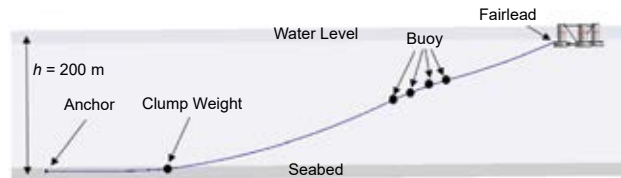


Figure 7. Mooring configurations containing buoys and a clump weight

mooring lines, are investigated. The results obtained from the statistical study of the platform response in a time domain duration of 2000 s and for a regular wave, with an amplitude of 5 m and a period of 12 s, are analyzed.

Figures 8 and 9 show the numerical results obtained for the OC4-DeepCwind and the four case studies used to investigate the effects of the buoys and clump weight on the global responses

Table 5. Buoys and clump weight properties

Buoy and CW Type	Buoy weight in water (kg)	Buoy (B2) diameter (m)	CW (P2) diameter (m)	CW (P2) weight (kg)
Type 1	34 330	4	0.84	5000
Type 2	17 165	3.17	0.84	5000
Type 3	11 443	2.77	0.84	5000
Type 4	8582	2.52	0.84	5000

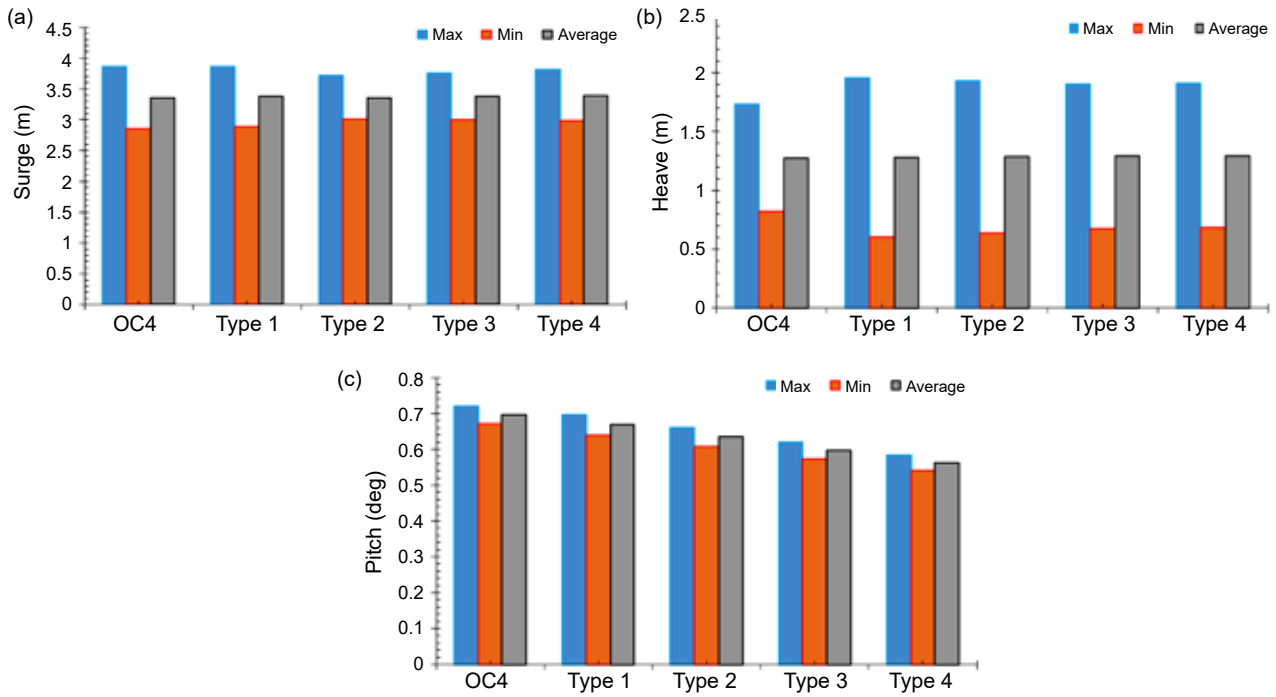


Figure 8. Time response of the motion (a) surge, (b) heave, and (c) pitch

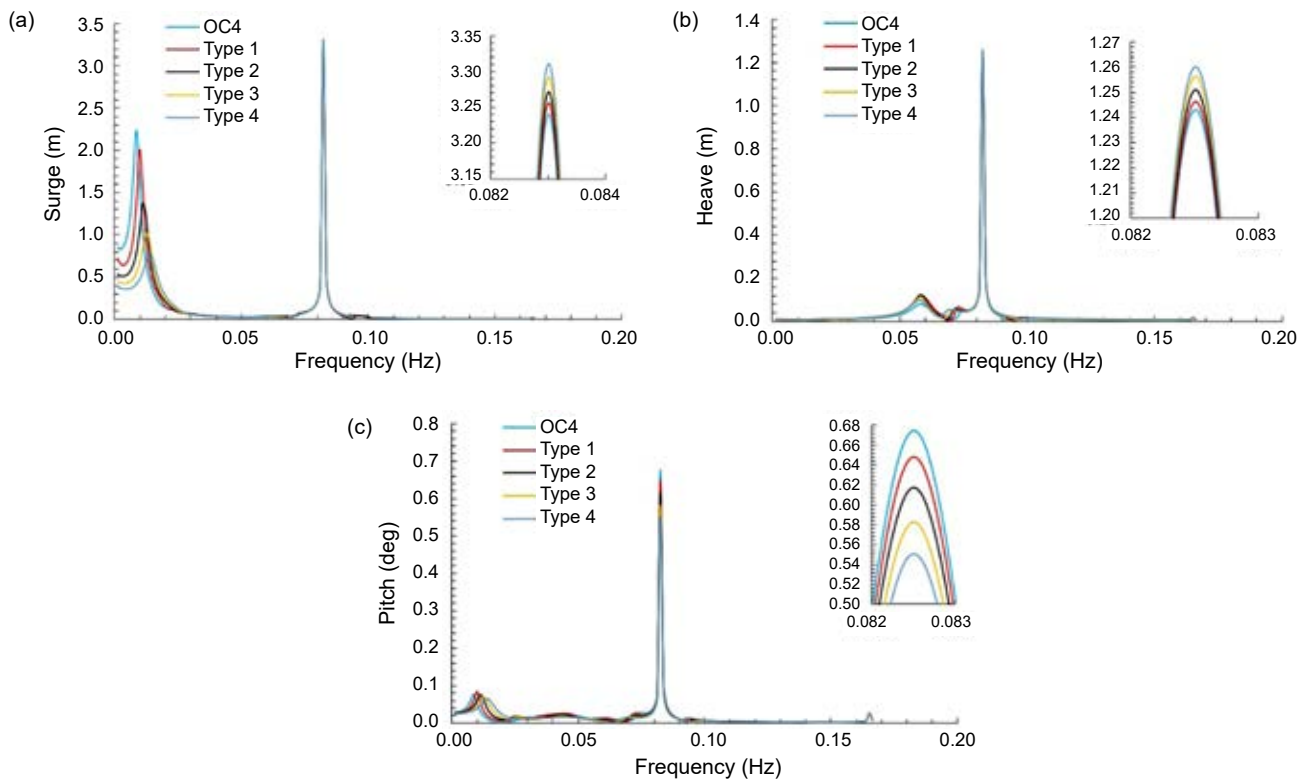


Figure 9. Frequency response of the motion (a) surge, (b) heave, and (c) pitch

of a semisubmersible platform, in the TDA and FDA.

As shown in Figure 8, it was found that by increasing the number of buoys (types 1–4) the amplitude of the surge and pitch motions, and the maximum, minimum, and average values, all decreased. Also,

for the heave motion, it can be seen that their amplitudes are slightly increased by escalating the number of buoy oscillations with maximum, minimum, and average values.

Figure 9 is determined from the FDA and shows that the surge and heave motions frequency response

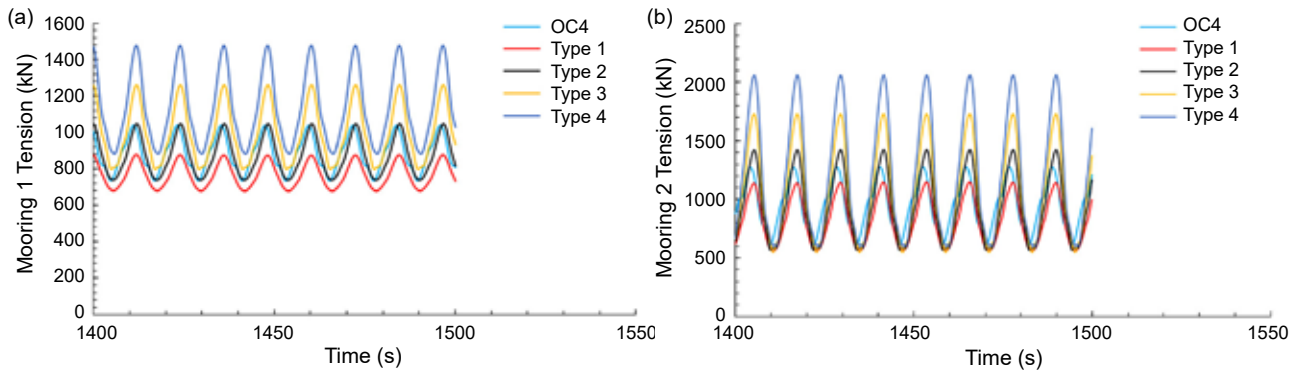


Figure 10. Time response of the fairlead tension responses for the (a) mooring line 1 and (b) mooring line 2

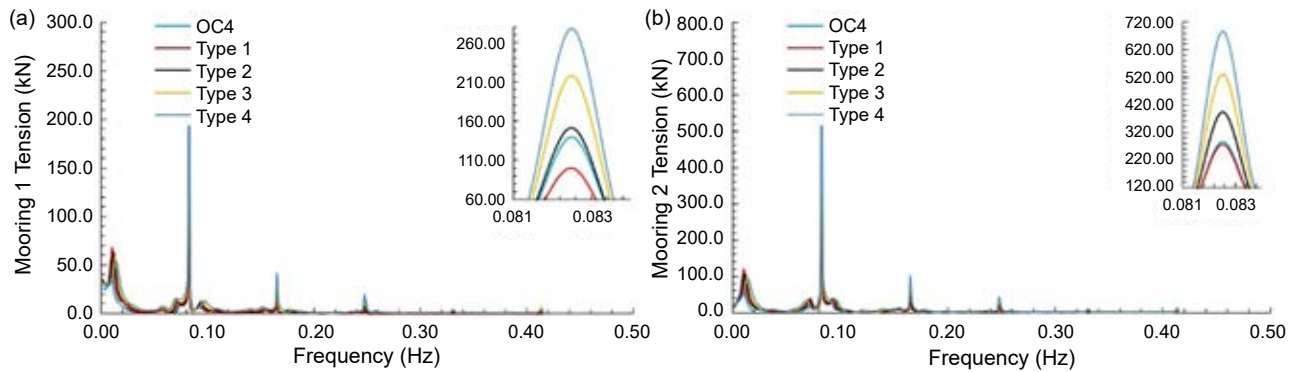


Figure 11. Frequency response of the fairlead tension responses for the (a) mooring line 1 and (b) mooring line 2

have two resonant frequencies. The low frequency decreases as the number of buoys increases, while the wave frequency response oscillation also increases. For the pitch motion, increasing the number of buoys means that the low and wave frequency decrease.

The tension force of the mooring line is shown in Figure 10. Here, by initially adding a buoy and clump weight (type 1) to the mooring line, the tension force of mooring lines 1 and 2 are decreased. Then, increasing the number of buoys in the constant volume escalates the oscillations of the tension force of mooring lines 1 and 2.

Figure 11 shows that adding buoy and clump weight may cause a decrease in the tension force of the mooring line. Besides, it can be seen that there are two resonant frequencies for the mooring tension. On increasing the number of buoys, the low

frequency oscillation decreases for the two mooring lines. The frequency oscillation of the resonant wave frequency for type 1 is reduced, while it is increased for a rising number of buoys with constant volume.

Case study type 1

This section considers five different regular waves for the type 1 case study. The response of the platform in the absence of wind was investigated using numerical results for surge, heave, and pitch response motions, and the mooring tension for the DeepCwind semisubmersible platform was due to wave excitation. Table 6 shows the selected sea states for the regular waves defined by period, T , and wave amplitude, A .

The amplitude oscillation of the surge, heave, and pitch motion for case study type 1 is shown in Figure 12, which is determined from the time response analysis. It was discovered that, by increasing the wave period for the five regular waves of constant amplitude, the amplitude of the surge maximum, minimum, and average value motion are enhanced. For the heave motion, it can be seen that with a growing wave period and constant amplitude, the oscillations of maximum, minimum, and average values all increased, except for a wave period of 14 s. Moreover, with an

Table 6. Environmental conditions of the five seas states

Regular wave	Amplitude (m)	Period (s)
Sea state 1	5	8
Sea state 2	5	10
Sea state 3	5	12
Sea state 4	5	14
Sea state 5	5	16

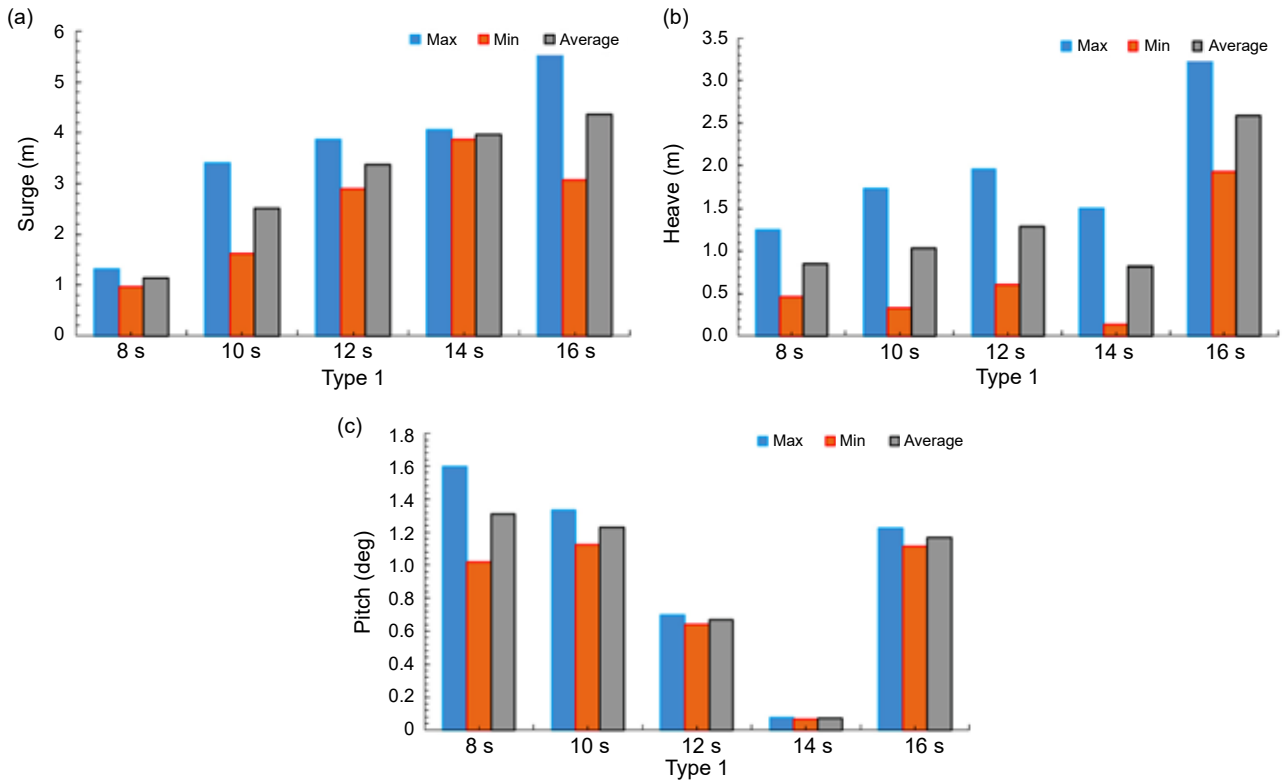


Figure 12. Time response of the motion (a) surge, (b) heave, and (c) pitch for type 1

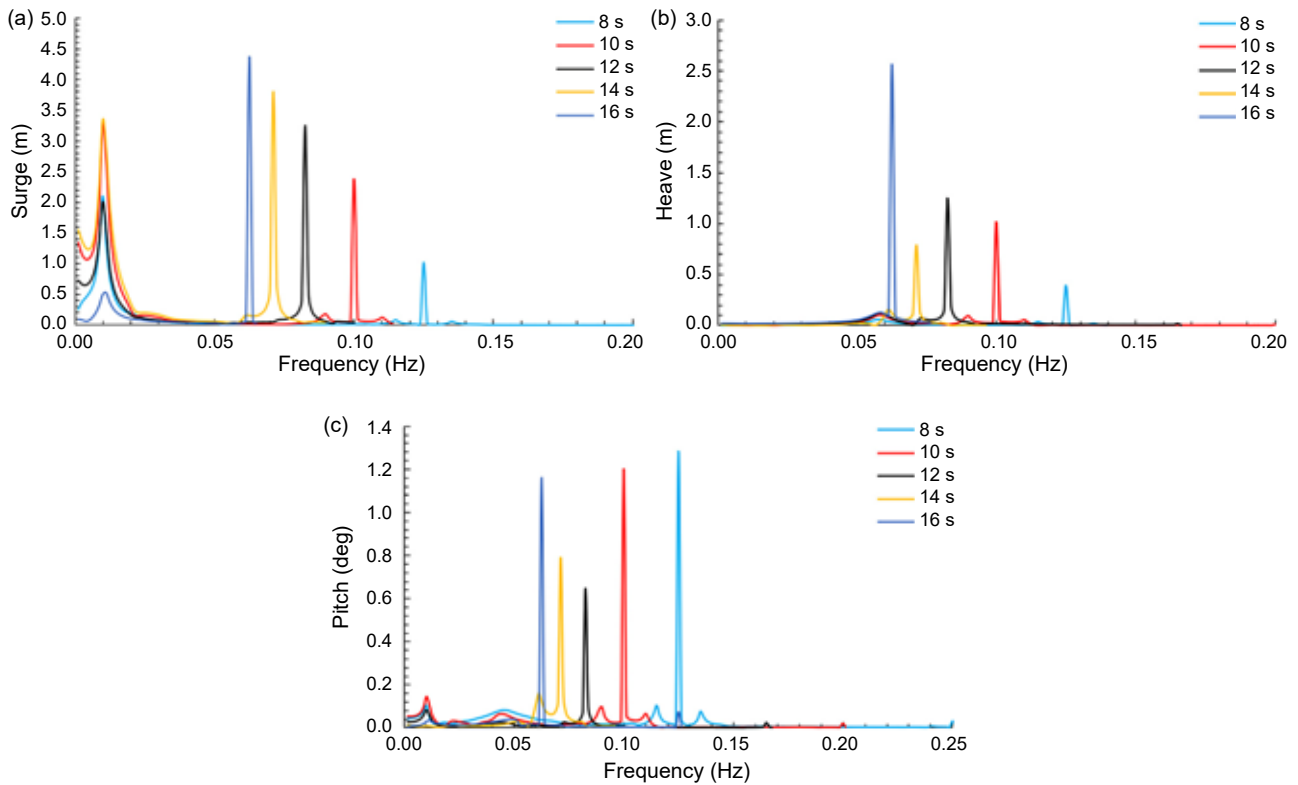


Figure 13. Frequency response of the motion (a) surge, (b) heave, and (c) pitch for type 1

increase in the wave period constant amplitude for the pitch motion, the oscillations of maximum, minimum, and average values decreased, except at a wave period of 16 s for which it increased.

Figure 13, determined from the FDA for case study type 1, shows that the surge and heave motions frequency response have two resonant frequencies. The lower frequency decreases as the wave period

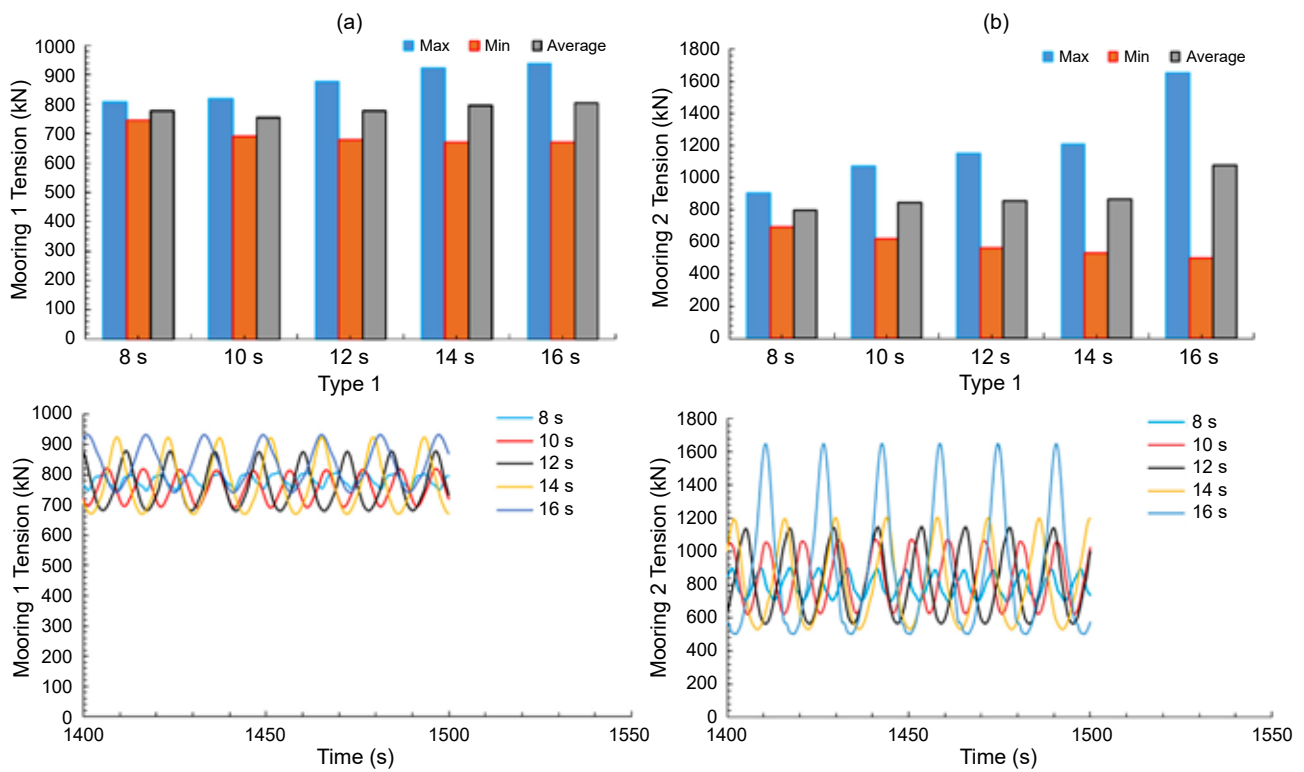


Figure 14. Time response of the fairlead tension responses for the (a) mooring line 1 and (b) mooring line 2 for type 1

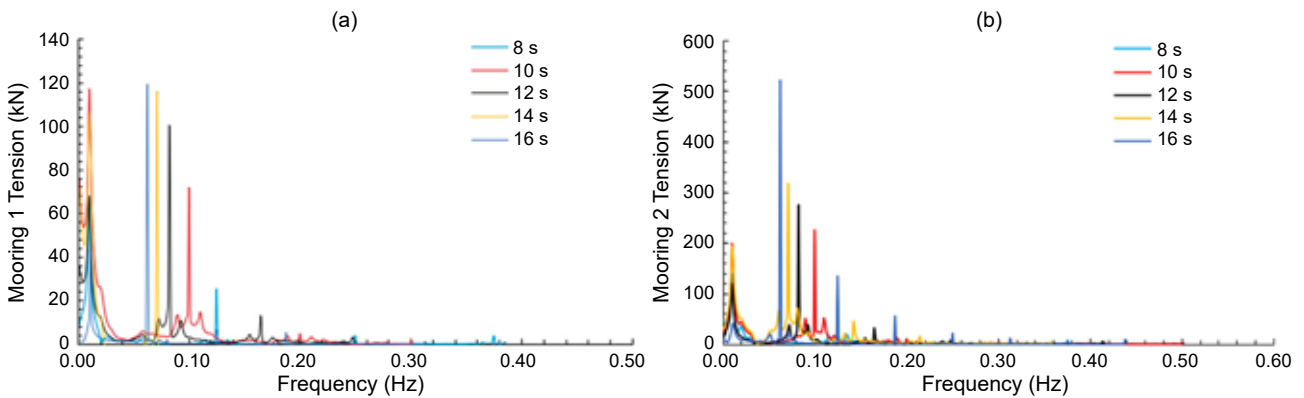


Figure 15. Frequency response of the fairlead tension responses for the (a) mooring line 1 and (b) mooring line 2 for type 1

(with a constant amplitude of 5 m) increases. Furthermore, the oscillation amplitude wave frequency increases, except for the heave motion of sea state 4. For the pitch motion, the wave period increases and the lower frequency decreases, and the wave frequency first decreases for sea states 1, 2, and 3 and then increases for sea states 4 and 5.

The tension force of the mooring line is shown in Figure 14 for case study type 1. Here, increasing the wave period for the five regular waves escalates the oscillation amplitude of the tension force of mooring lines 1 and 2.

Figure 15 shows a different regular wave with a constant amplitude for the tension force of the mooring lines. It can be seen here that there are

two resonant frequencies for the mooring tension. The lower frequency oscillation decreases with an increasing wave period, and the wave frequency oscillation amplitude grows.

Conclusions

The effects of the buoys and clump weight on the mooring line tension and platform responses were investigated for surge, heave, and pitch motions of the DeepCwind semisubmersible floating platform, for regular wave conditions. The BEM method was used to simulate the hydrodynamic responses of the platform in both the FDA and TDA. It was found that on increasing the number of buoys (types

1–4), the amplitude of the surge and pitch motions decreased, while for the heave motion it grew. Adding a buoy and clump weight (type 1) to the mooring line reduced its oscillation tension force, while raising the number of buoys in the constant volume increased this force. For the surge and heave motions, the oscillation of the resonant lower frequency is decreased as the number of buoys increases but it is the opposite for the wave frequency. In addition, for the pitch motion, both of them are reduced. In the case of type 1, raising the wave period for the five sea states increases the amplitude of the surge and heave motions, except for the heave motion of state 4. Furthermore, the oscillation amplitude decreased for the pitch motion, except in sea state 5 for which it increased. Additionally, when the oscillation of the mooring tension has an enhanced wave period, the lower frequency amplitude is reduced and the wave frequency amplitude is increased.

References

1. BARLTROP, N.D.P. (Eds.) (1998) *Floating Structures – A guide for design and analysis. Volume 1*. Energy Institute.
2. BENASSAI, G., CAMPANILE, A., PISCOPO, V. & SCAMARDELLA, A. (2014) Mooring control of semisubmersible structures for wind turbines. *Procedia Engineering* 70, pp. 132–141, doi: 10.1016/j.proeng.2014.02.016.
3. BROMMUNDT, M., KRAUSE, L., MERZ, K. & MUSKULUS, M. (2012) Mooring system optimization for floating wind turbines using frequency domain analysis. *Energy Procedia* 24, pp. 289–296, doi: 10.1016/j.egypro.2012.06.111.
4. COULLING, A.J., GOUPEE, A.J., ROBERTSON, A.N., JONKMAN, J.M. & DAGHER, H.J. (2013) Validation of a FAST semisubmersible floating wind turbine numerical model with DeepCwind test data. *Journal of Renewable and Sustainable Energy* 5, 023116, doi: 10.1063/1.4796197.
5. CUMMINS, W.E. (1962) The impulse response function and ship motions. *Schiffstechnik* 9, pp. 101–109.
6. GHAFARI, H. & DARDEL, M. (2018) Parametric study of catenary mooring system on the dynamic response of the semisubmersible platform. *Ocean Engineering* 153, 1, pp. 319–332, doi: 10.1016/j.oceaneng.2018.01.093.
7. GHAFARI, H.R., KETABDARI, M.J., GHASSEMI, H. & Homayoun, E. (2019) Numerical study on the hydrodynamic interaction between two floating platforms in Caspian Sea environmental conditions. *Ocean Engineering* 188, 106273, doi: 10.1016/j.oceaneng.2019.106273.
8. HALL, M. & GOUPEE, A. (2015) Validation of a lumped-mass mooring line model with DeepCwind semisubmersible model test data. *Ocean Engineering* 104, pp. 590–603, doi: 10.1016/j.oceaneng.2015.05.035.
9. HORDVIK, T. (2011) *Design analysis and optimisation of mooring system for floating wind turbines Student: Open Floating wind turbine Mooring system Optimisation*. Master Thesis. Norwegian University of Science and Technology. [Online]. Available: <https://core.ac.uk/download/pdf/52099634.pdf> [Accessed: May 14, 2022].
10. LI, J., JIANG, Y., TANG, Y., QU, X. & ZHAI, J. (2017) Effects of second-order difference-frequency wave forces on floating wind turbine under survival condition. *Transactions of Tianjin University* 23, pp. 130–137, doi: 10.1007/s12209-017-0037-2.
11. LIU, Z., TU, Y., WANG, W. & QIAN, G. (2019) Numerical analysis of a catenary mooring system attached by clump masses for improving the wave-resistance ability of a spar buoy-type floating offshore wind turbine. *Applied Science* 9, 1075, doi: 10.3390/app9061075.
12. MAVRAKOS, S.A. & CHATJIGEORGIOU, J. (1997) Dynamic behaviour of deep water mooring lines with submerged buoys. *Computers & Structures* 64, pp. 819–835, doi: 10.1016/S0045-7949(96)00169-1.
13. MAVRAKOS, S.A., PAPAZOGLU, V.J., TRIANTAFYLLOU, M.S. & BRANDO, P. (1991) *Experimental and numerical study on the effect of buoys on deep water mooring dynamics*. The First International Offshore and Polar Engineering Conference. Edinburgh, UK. [Online]. Available: <https://onepetro.org/conference-paper/ISOPE-I-91-098> [Accessed: May 14, 2021].
14. MOTALLEBI, M., GHAFARI, H.R., GHASSEMI, H. & SHOKOUHIAN, M. (2020) Calculating the second-order hydrodynamic force on fixed and floating tandem cylinders. *Scientific Journals of the Maritime University of Szczecin, Zeszyty Naukowe Akademii Morskiej w Szczecinie* 62, pp. 108–115, 2020, doi: 10.17402/425.
15. QIAO, D. & OU, J. (2013) Global responses analysis of a semisubmersible platform with different mooring models in South China Sea. *Ships and Offshore Structures* 8, pp. 441–456, doi: 10.1080/17445302.2012.718971.
16. VICENTE, P.C., FALCÃO, A.F. & JUSTINO, P.J. (2011) *Slack-chain mooring configuration analysis of a floating wave energy converter*. In Proceedings of the 26th International Workshop on Water Waves and Floating Bodies, Thessaloniki, Greece (Vol. 17). Available: http://www.iwwwfb.org/Abstracts/iwwwfb26/iwwwfb26_50.pdf [Accessed: May 14, 2022].
17. YUAN, Z.-M., INCECIK, A. & JI, C. (2014) Numerical study on a hybrid mooring system with clump weights and buoys. *Ocean Engineering* 88, pp. 1–11, doi: 10.1016/j.oceaneng.2014.06.002.

Cite as: Ganjgani, A.A., Ghassemi, H., Ghiasi, M. (2022) Investigation into a hybrid mooring system with hydrodynamic response and mooring tension from a DeepCwind floating wind turbine. *Scientific Journals of the Maritime University of Szczecin, Zeszyty Naukowe Akademii Morskiej w Szczecinie* 71 (143), 11–21.